

# Analysis of the vibration structure of a hypocenter using a singular value decomposition method

\*Toshiaki Kikuchi<sup>1</sup>

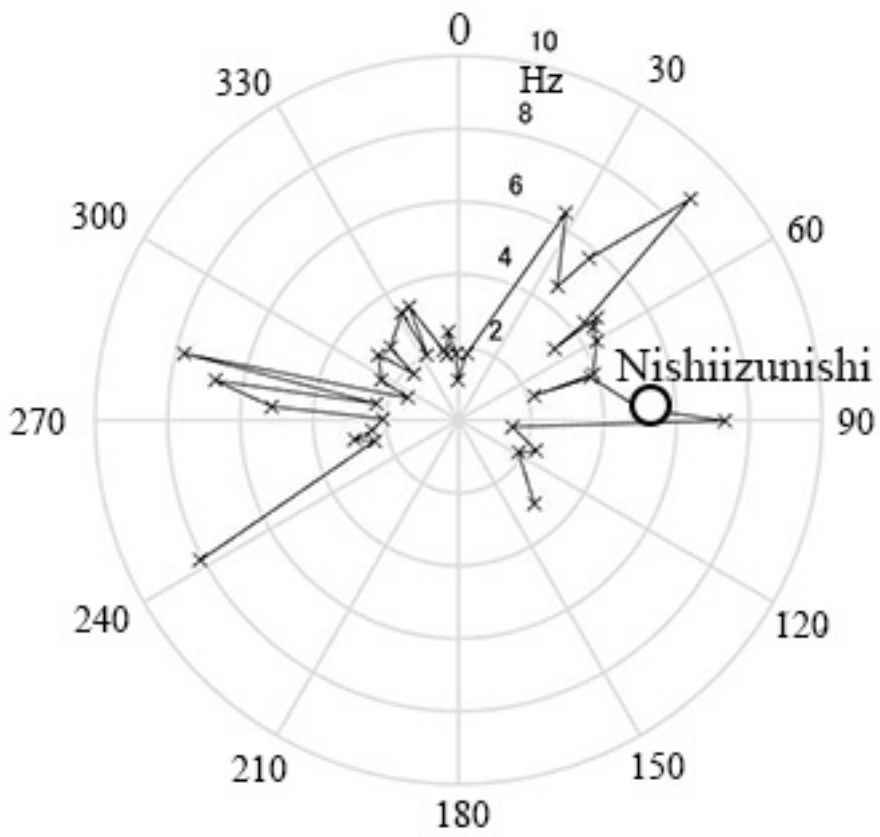
1. National Defense Academy

The vibration structure of a hypocenter are analyzed using a singular spectrum analysis. Specific radiation characteristics related to a hypocenter structure from the results become apparent. The specific radiation characteristics are confirmed for five earthquakes including Kumamoto earthquake. The analysis process is carried out in two stages of the acquisition of equivalent hypocenter vibrations using a time reversal method and the singular spectrum analysis of acquired hypocenter vibration. First, a P wave is cut out from a seismic wave received at an observation station surrounding a hypocenter, and the signal obtained by inverting the time axis of the signal is radiated on a propagation simulation to obtain a pulse formed at the hypocenter position.

At this time, a propagation environment is changed to obtain the condition that the amplitude of a pulse becomes maximum, and the condition is set as the optimum propagation environment. Next, a time reversal pulse (TRP) that is, equivalent hypocenter vibration obtained on the best propagation environment, is analyzed. Since the TRP is a complex oscillating nonlinear signal consisting of multiple frequencies, it is analyzed using a singular value decomposition method. The matrix of time interval  $dt$  that consists of  $n$  points that consists of the TRP corresponding to an observation station is created. Next, the second matrix that delayed the entire matrix by  $dt$  is created. In addition, the third matrix that delayed second matrix by  $dt$  is created. This process is repeated  $m$  times to obtain a matrix of  $m \times n$ . The final matrix is an orbital matrix  $\mathbf{X}$ . Singular value  $W$  is obtained solving the following expression,  $\mathbf{X} = \mathbf{U}\mathbf{W}\mathbf{V}^T$ . Here,  $\mathbf{U}$  and  $\mathbf{V}$  are orthonormal matrices satisfying the equation,  $\mathbf{U}^T\mathbf{U} = \mathbf{V}^T\mathbf{V} = \mathbf{E}$  ( $\mathbf{E}$ : unit matrix). The largest singular value in the  $W$  is assumed to be a main component. Here, the earthquake of M6.5 that occurred in the southern part of Suruga Bay on August 11, 2009 was analyzed. First, a P wave is cut out from a signal received at the observation station located around Suruga Bay, and the time axis of the signal is reversed. The reversed signal are radiated from the observation station on the propagation simulation and the pulse (TRP) at the hypocenter location is formed. The singular value decomposition method is applied to the TRP to calculate the components constituting the pulse, and the component with the largest amplitude among them is obtained. The determined main component is a gently fluctuating pulse consisting of almost a single frequency. Likewise, the singular value decomposition method is applied to the TRP corresponding to each observation station, and the component with the largest amplitude is extracted. The frequencies of these components are shown in the figure as a distribution to the azimuth of observation stations centered on the hypocenter. Obviously, the radiation frequency from the hypocenter shows a directivity greatly different depending on the azimuth. That is, the frequency from Susono with the azimuth of  $27.4^\circ$  to Kawadu with the azimuth of  $97.0^\circ$  is high.

These radiation patterns are considered to be related to the vibration mode of active faults.

Keywords: Hypocenter vibration, Time reversal method, Singular value decomposition



# The summary of Wave Features Theory of 2011.2.NZ Earthquake Motion.(The same as URAYASU CITY of The TOHOKU Great, The 1964 NIIGATA Earthquake.)

\*Masaru Nishizawa<sup>1</sup>

1. none

I . PREFACE: had summarized wave features theory of 2011.2.NZ Earth quake Motion. In this area, many seismoments are mstalled. As a result, 9easily summarized wave features theory. City of the 2011 TOHOKU Great Earthquake and The 1964 NIIGATA Earthquake.

## II . The Wave Features Theory

(1) V(vertical)this wave features are closely related to the normal wave features. A and B wave features appears soft ground states.

(2) The excellent period is about 0.2 sec, therefore  $f=1/f$  this fregurency is high considerably. But the period of the A and B is 4 or 5 times.

(3) The fregurencie of V in completely different from A, B. As thus result, phase shift gres rise to amatter of course. On the CTV building, some supernatural power seems to be at work.

In this short, the complicated oscillation and sotation (twis acr on bwdings, moreover coming ont top of Rayleigh wave actions.

(4) The horizontal rayleigh wave features shows many reversal of phase. As a result, the building satate on an vential axis. This setation (twist) is very important force. Of course, CTV building. (Reference. Masaru NISHIIZAWA : The strong spectrum of resemblance between frontier spectrum and Phase difference spectrum of the seismic wave. (Science of form) 2016, JpGU,S-SS25-P35.

This notation force is one of the importance pf the phase spectrum.

(5) (+)Acceleration and (-)Acceleration indicates different values. Namely, A,B,U acceleration together (+)acceleration indicates higher values than (-) one. This fact indicates the existence of the firm ground than the appear ground. This is the difference of the reflection between firm and soft ground.

(6) I Think that the thickness of the soft ground in soft is not all by my fair judgment by observing wave features of the soft ground.

(7) The same distance from the center from the center of the earthquake, though the time of arrival in exists different observation point . This reason is that the speed of the wave of soft ground in slow generally than the firm one.

Abstract:

Because of soft ground, Phase of seismic wave devided from correct behavior and generated rotation (twist) arownd CTV Building (the buildings).

This factor of this rotation (twist) in the phase shift or reversal of phase. This is one of the importance of the phase spectrum.

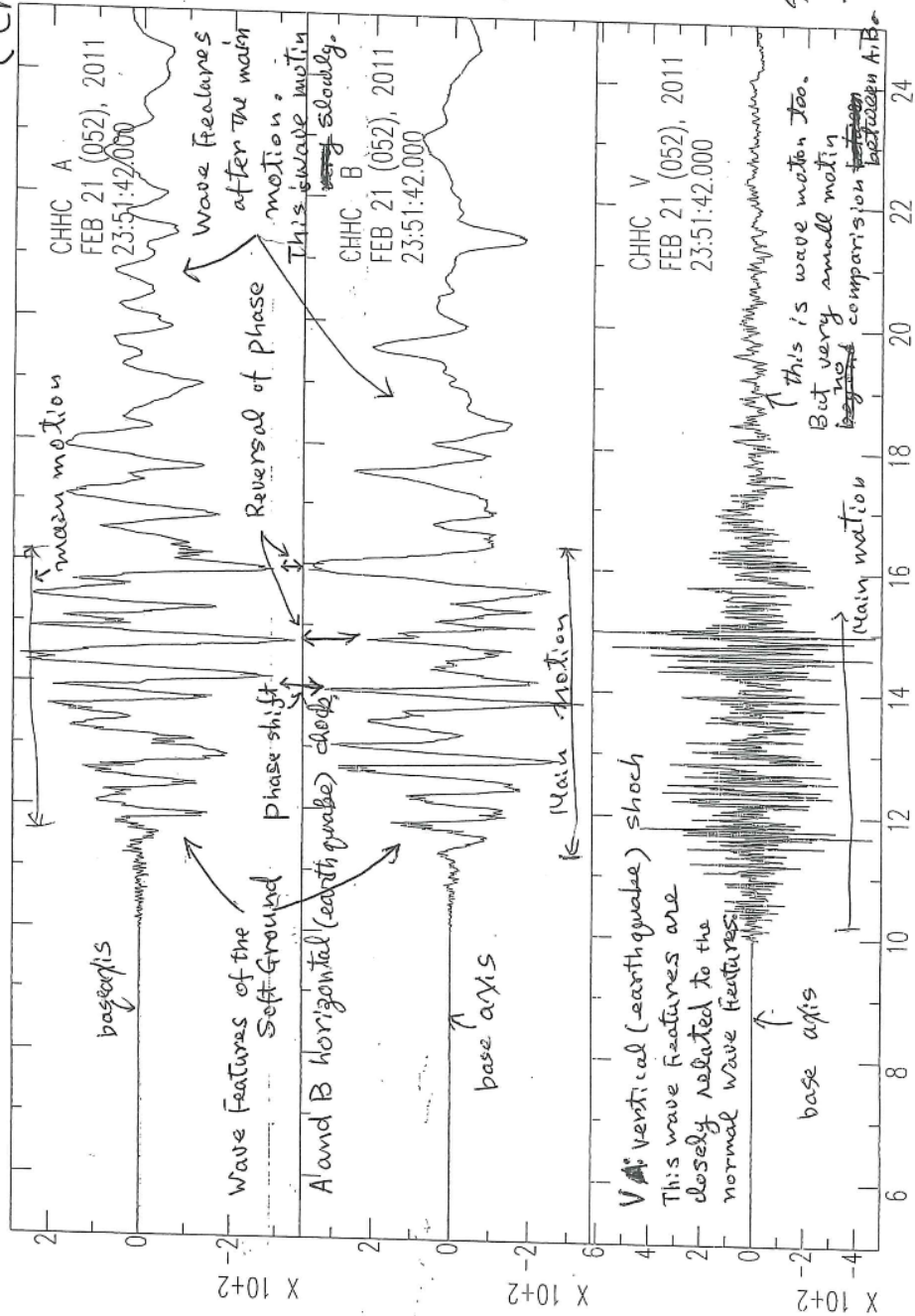
The wave Features of Christchurch.

73 仅 A  
(Christchurch)  
の波形状  
(Wave features)

の主要な特徴は、  
波の位相は逆転  
している。これは他と同  
じで、水圧反動に  
よるもの。これに、回転  
力(又はトルク)が加  
わると、より複雑な

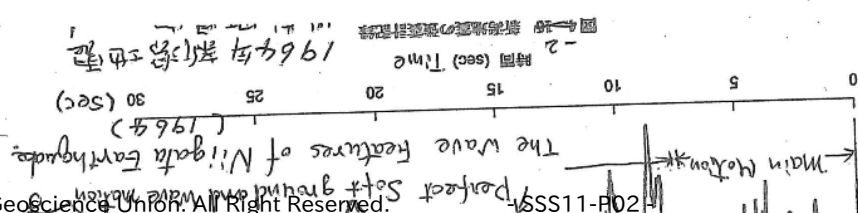
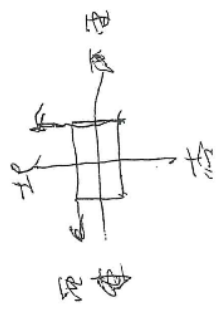
の主要な特徴は、  
波形状は波の位相  
の逆転は他と同  
じである。

しかし、上下方向も  
多少は波の位相逆  
転が、重複して発生  
しているように見  
える。



(+) amount of SA, B, V acceleration is high (震央距離 8 km)

than (-) amount acceleration.  
This fact point out existence of a hard type of the ground  
than this soft ground. And this soft ground  
is not thickly layered, particularly thick.





# Surface wave characteristics from ambient seismic noise in Northern China

\*Yiqiong Li<sup>1</sup>

1. Institute of Geophysics, China Earthquake Administration

Studies have shown that the western Taiwan coastal plain is influenced by long-period ground motion from the 1999 Chi-Chi, Taiwan, earthquake, and engineering structures with natural vibration long-period are damaged by strong surface wave in the western coastal plain. The thick sediments in the western coastal plain are the main cause of the propagation of strong long-period ground motion. The thick sediments similar to in the western coastal plain also exist in northern China.

It is necessary to research the effects of thick sediments to long-period ground motion in northern China. We extract surface wave from ambient seismic noise in Northern China and analyze frequency spectrum of surface wave. Our purpose is to reveal the formation and propagation of long-period surface wave in thick sediments and to grasp the amplification effect of long-period ground motion due to the thick sediments.

Keywords: Surface wave, Ambient seismic noise, Thick sediments

## Relationship between P wave velocity change and pore water pressure variation induced by the 2016 Kumamoto Earthquake

\*Takahiro Kunitomo<sup>1</sup>, Hiroshi Ishii<sup>1</sup>, Yasuhiro Asai<sup>1</sup>

1. Tono Research Institute of Earthquake Science, Association for the Development of Earthquake Prediction

We developed a compact seismic source suitable for high frequency underground survey with the use of the giant magnetostrictive actuator (GMA). This giant magnetostrictive seismic source is composed of a controller system and a vibration exciter driven by a GMA. The controller system generates driving current for a GMA with arbitrary wave form in synchronization with a GPS clock. The vibration exciter generates single force in vertical direction with maximum generating force of 91kgf. This system is currently used to observe mainly P wave velocity change of the bedrock (Toki granite) in 100-200Hz frequency range, because the sampling frequency of the A/D converter in the comprehensive borehole crustal activity observation device is 400Hz. Even at observation points 700m away from the seismic source, it is possible to observe changes in P wave travel time with accuracy of about  $10 \mu\text{s}$  by stacking for 1 day.

Stepwise travel time delay of the direct P wave, induced by the Kumamoto earthquake (April 16, 2016, Mj7.3), is observed at TGR 350 (distance 353m, about  $25 \mu\text{s}$  delay) and TRIES (distance 690m, about  $60 \mu\text{s}$  delay) shortly after the start of continuous transmission. These travel time delays are thought to be caused by the decrease in P wave velocity due to opening cracks in Toki granite. Coseismic and postseismic travel time change of the direct P wave detected at TRIES is consistent with the long-term fluctuation pattern of pore water pressure observed at STG200N in the shaft of the Mizunami Underground Research Laboratory (JAEA). The pore water pressure in the granite rose gradually after stepwise rising at the time of the earthquake, peaked at the beginning of June (about 30kPa), and then gradually dropped. Direct P wave travel time is delayed gradually after the stepwise delay on the day of the earthquake, delayed to about  $90 \mu\text{s}$  at the same time as the pore water pressure peak, and then gradually recovered. If the pore water pressure rise of 10kPa is converted into the travel time delay of  $30 \mu\text{s}$ , they coincide with each other within the margin of the travel time change estimated error over several months. This result indicates that the pore water pressure changes in the Toki granite controls the opening and closing of the crack and the P wave velocity changes.

Keywords: giant magnetostrictive seismic source, P wave velocity change, pore water pressure, crack, granite

## Detection of the changes in elastic wave characteristics in the model slope before and during shallow landslides

\*Issei Doi<sup>1</sup>, Hironori Kawakata<sup>2</sup>, Masayuki Nakayama<sup>2</sup>, Naoki Takahashi<sup>3</sup>, Takahiro Kishida<sup>4</sup>

1. Disaster Prevention Research Institute, 2. College of Science and Engineering, Ritsumeikan University, 3. SUMITOMO MITSUI CONSTRUCTION CO., LTD, 4. SMC Tech.

In order to reduce the damages due to shallow landslides, it is effective to construct an early warning system. We pay attention to the use of elastic waves which was used for the rock behavior before the main rupture (Yoshimitsu et al., 2009; Yoshimitsu and Kawakata, 2011). As a first step, we conducted a model test for propagation characteristics of elastic waves before and during shallow landslides.

Landslides occurred 4, 23, and 26 minutes after the initiation of the experiments. The travel times of the elastic waves got larger at the starting time of precipitation and ten minutes before one landslide. These facts suggest that it is possible to monitor the moisture situation and the small deformation of the slope using elastic waves.



## Application of seismic interferometry to attenuation estimation on zero-offset vertical seismic profiling data

\*Jun Matsushima<sup>1</sup>, Mohammed Y. Ali<sup>2</sup>, Fateh Bouchaala<sup>2</sup>

1. School of Engineering, The University of Tokyo, 2. The Petroleum Institute, Abu Dhabi

Although seismic attenuation measurements have great potential to enhance our knowledge of physical conditions and rock properties, their application is limited because robust methods for improving both the resolution and accuracy of attenuation estimates have not yet been established. In general, it is difficult to improve both the resolution and accuracy of attenuation estimates because there is a relationship of trade-off between them. Thus, the development of a robust method for improving both the resolution and accuracy of attenuation estimates is important. A zero-offset VSP measurement is considered to be best suited for attenuation studies as it enables sampling of the downgoing wavefield at various known depths because the downgoing waveform in a zero-offset VSP data set provides direct observations of the changing nature of the source wavelet as it propagates through the Earth. We propose attenuation estimation methods for zero-offset vertical seismic profile (VSP) data by combining seismic interferometry (SI) and the modified median frequency shift (MMFS) method developed for attenuation estimation using sonic waveform data. One important advantage of the application of SI to seismic exploration is that it allows flexibility of the source and receiver configurations. For example, this means that by applying SI to two different seismic traces recorded at different receivers, a new seismic trace with one receiver acting as a source (virtual source) and the other acting as a receiver can be created. The configuration of zero-offset VSP data is redatumed to that of the sonic logging measurement by adopting two types of SI: deconvolution interferometry (DCI) and crosscorrelation interferometry (CCI). Then, we can apply the MMFS method to the redatumed VSP data. Although the amplitude information estimated from CCI is biased, we propose a correction method for this bias to correctly estimate attenuation. First, to investigate the performance both in resolution and accuracy, we apply different trace separations to synthetic data with random noise at different signal-to-noise ratio (SNR) levels. Second, we estimate the influence of residual reflection events after wavefield separation on attenuation estimation. The proposed methods provide more stable attenuation estimates in comparison with the spectral ratio (SR) method because the mean-median procedure suppresses random events and characteristic features caused by residual reflection events in spectral domain. Our numerical experiments also demonstrate that the MMFS methods identify impulsive attenuation values caused by transmission loss due to reflection at an interface while such impulsive values are not observed in SR methods. This is because the SR method derives attenuation estimates based on frequency component change between two receiver depths while the MMFS method uses the amplitude variation, implying that the proposed methods can estimate scattering attenuation values from amplitude information even if frequency components are not changed between the two receiver depths. By preliminarily applying the proposed methods to field VSP data, we find some differences in the depth resolution and stability of attenuation values between the proposed method and the SR method, demonstrating that the proposed methods are more stable than the SR method especially in the shortest receiver separation. The responses of attenuation results obtained by applying different attenuation estimation methods to field data at different receiver separations correlate with those in our numerical experiments. To further verify and extend the applicability of the proposed method, one of future works should focus on validation of obtained attenuation results by comparing a seismic trace or its spectrum before and after attenuation compensation by inverse  $Q$  filtering. In our case, a component of attenuation due to scattering effects is also included in the obtained attenuation estimates and thus such scattering effects should be taken into account in attenuation compensation.

This attenuation compensation process might be used to estimate the scattering effects. To this end, a study to further investigate the response of the proposed methods to seismic scattering effects which are frequency dependent could be useful in providing new perspectives on the usage of the proposed method.

Keywords: Seismic interferometry , Seismic attenuation, zero-offset VSP

## Approximate vector sensitivity kernels of coda-wave decorrelation: 2D single scattering

\*Hisashi Nakahara<sup>1</sup>, Kentaro Emoto<sup>1</sup>

1. Solid Earth Physics Laboratory, Department of Geophysics, Graduate School of Science, Tohoku University

Coda-wave interferometry has been used to detect medium changes in association with large earthquakes or volcanic eruptions. It is important to determine the region of these medium changes correctly for understanding physical mechanisms to cause them. For that purpose, sensitivity kernels of coda waves play a crucial role. Regarding travel time changes of coda waves, the sensitivity kernels have been approximately extended to vector waves under single scattering regime by Nakahara and Emoto (2016). Regarding decorrelation of coda waves, the sensitivity kernels have been formulated so far for scalar waves only (e.g. Planes et al, 2014; Margerin et al., 2016). Hence, we try to derive analytical expressions for vector waves in two-dimensional cases. The key point in our simple extension to vector waves is the projection of seismic phonon energy into horizontal and vertical components by using the square of the direction cosine of the polarization direction. This idea is the same as one used in Nakahara and Emoto (2016) for travel-time sensitivity kernels. Thanks to this simple idea, we can derive approximate but analytical expressions of the sensitivity kernels by using the two-dimensional single isotropic scattering model for scalar waves, though we can treat either P waves or S waves at a time. Our results show that the sensitivity kernels are different for different components. They have non-zero values only on the single-scattering shells. There exist points where the kernels have zero amplitudes, and these points are different for the two components. These are theoretically shown by this study for the first time. These sensitivity kernels are helpful for us to know how to use different components simultaneously in coda-wave interferometry.

Keywords: Sensitivity kernel, coda waves, vector waves

## Estimation of scattering coefficient and intrinsic absorption in the Chugoku district (2)

Daisuke Takahagi<sup>1</sup>, \*Jun Kawahara<sup>1</sup>, Kentaro Emoto<sup>2</sup>, Tatsuhiko Saito<sup>3</sup>

1. Ibaraki University, 2. Tohoku University, 3. National Research Institute for Earth Science and Disaster Resilience

It is possible to separately estimate the scattering coefficient and intrinsic absorption of the lithosphere by interpreting the observed spatiotemporal distribution of high-frequency seismic wave energy by the Radiative Transfer Theory (RTT). One of such an estimation method is the Multiple Lapse-Time Window (MLTW) method (Fehler et al., 1992; Hoshiya, 1993; Carcole and Sato, 2010), in which the seismic wave energy observed respectively at different positions is integrated using multiple time windows and then its spatial variation is interpreted by the RTT. Recently, Saito et al. (2013, 2014, Seism. Soc. Jp. Fall Meet.) proposed another method to estimate the scattering coefficient and intrinsic absorption. In this method, the seismic wave energy observed respectively at different times is integrated using multiple space windows and then its temporal variation is interpreted by the RTT. Sasaki et al. (2015a, JpGU Meet.; 2015b, SSJ Fall Meet.) improved this method and applied it to the Hi-net records of several shallow earthquakes in the Chugoku district, Japan. He concluded that the scattering coefficient of S waves (1-2 Hz) in this region is on average 0.002-0.0025 km<sup>-1</sup>. It is roughly half as large as the values previously estimated in this region using the MLTW method.

In this study, we improved the coda normalization process for correcting the source and site effects in the method of Sasaki et al. Though they assumed that the scattering coefficient ( $g_0$ ) and intrinsic absorption ( $Q_i^{-1}$ ) are uniform, we introduced a model such that the crust and the uppermost mantle could have  $g_0$  and  $Q_i^{-1}$  of different values. We analyzed the Hi-net data of the same events using the improved method. We obtained the  $g_0$  and  $Q_i^{-1}$  for frequency bands of 1-2, 2-4, and 4-8 Hz. The  $g_0$  did not show obvious frequency dependence, but the  $Q_i^{-1}$  appeared smaller for higher frequencies. The  $g_0$  values we estimated were significantly smaller than those estimated by the previous studies using the MLTW method for all frequency bands. The choice of  $g_0$  and  $Q_i^{-1}$  of the uppermost mantle gave little influence on the results. This is because the ray paths from the shallow events (9-13km in depth) that we selected mostly go through the crust only. To evaluate the  $g_0$  and  $Q_i^{-1}$  of the uppermost mantle, we would need to analyze data of deeper events.

Acknowledgements: We used the data by the Hi-net and the dataset of the velocity structure model of Matsubara and Obara (2011), both provided by National Research Institute for Earth Science and Disaster Resilience.

Keywords: seismic wave energy, scattering, intrinsic absorption

## Temporal change of subsurface structure near Mt. Aso inferred from seismic interferometry using V-net vertical array data

\*Yuta Mizutani<sup>2</sup>, Kiwamu Nishida<sup>1</sup>, Yosuke Aoki<sup>1</sup>

1. Earthquake Research Institute, University of Tokyo, 2. Univ. of Tokyo

Volcanic activity could be often activated by tectonic stress changes by a large earthquake. For example, Mt. Aso erupted in October 2016 after the 2016 Kumamoto Earthquake. To understand the relation between these events, it is important to monitor the temporal change of the structure of seismic velocity related to the event. In this study, we estimated the temporal change of subsurface structure in the Aso region with seismic interferometry (SI).

Monitoring seismic velocity by SI requires the isotropic source distribution, because the temporal or spatial change of the distribution of the sources biases the measured temporal change of subsurface structure. In order to mitigate the bias, a measurement of the temporal velocity change utilizing coda part of the cross-correlation function (CCF) is feasible. Moreover, the delay time of coda waves is larger than that of the direct waves. This means even a subtle change could be detected from coda waves with high accuracy. Here, we focused on how to localize the temporal subsurface velocity change from the difference between direct waves and coda waves.

In this study, we analyzed the data recorded from January 1, 2015, to October 31, 2016, at 4 V-net stations deployed by National Research Institute for Earth Science and Disaster Resilience (NIED) around Mt. Aso. Each station is composed of a broadband seismometer at the surface and a high-frequency seismometer (1 Hz) at the bottom of a borehole (depth  $\sim 200$  m). First, the records were bandpass-filtered from 2 to 8 Hz. After one-bit normalization of the records and spectral whitening, a CCF between same components of the bottom and surface sensors was calculated every day. Then, we made a reference CCF by stacking CCFs from October 25, 2016 to October 31, 2016. Second, we measured the delay times between the reference and a CCF in time windows of 2.56 s whose center time was increased from -5 s to 5 s every 0.2 s. Plots of the delay time against lag time show a linear trend. When the temporal change is homogeneous, the slope characterizes the bulk velocity change within a spatial scale of about 2 km. In contrast, the intercept, which represents travel time of direct waves, characterizes the localized velocity change between the station pair ( $\sim 200$  m).

After the 2016 Kumamoto Earthquake, the estimated slope of the EW component showed the velocity reduction of approximately 0.2 % at 3 stations except for Takamori station. At Takamori station, the seismic velocity was little changed in the EW component, but in the NS component, about 0.2 % of the velocity drop was detected. On the local velocity change in the borehole with the depth of about 200 m, nearly 5-8 % velocity drop was observed in the EW component at Hakusui and Ichinomiya stations and the NS component at Takamori station. Otherwise, there was an approximately 20 % drop at Nagakusa station. This could attribute the serious damage of subsurface structure by the earthquake.

At Ichinomiya station, the velocity change with a time scale of a few weeks coincided with that of the precipitation data. This change was well agreed with a simple model of the ground water level inferred from the data. The change could be localized near the borehole, because the detected temporal change was associated with that of water head in a volcanic alluvial fan.

In this study, we detected the temporal velocity change on a scale from several hundred meters to some kilometers using vertical array data. In a future study, we will address CCF analysis with ray paths across Mt. Aso for detecting the temporal change associated with the volcanic event.

Keywords: Seismic interferometry, Temporal change of seismic velocity

# Temporal change of subsurface velocity structure associated with the 2016 Kumamoto earthquakes

\*Tomotake Ueno<sup>1</sup>, Tatsuhiko Saito<sup>1</sup>, Kaoru Sawazaki<sup>1</sup>, Katsuhiko Shiomi<sup>1</sup>

1. National Research Institute for Earth Science and Disaster Resilience

We investigated temporal velocity change of subsurface structure before and after the 2016 Kumamoto earthquakes in April 2016 by applying the seismic interferometry method to ambient seismic noise. We calculated auto-correlation functions (ACFs) of continuous waveforms recorded by Hi-net vertical velocity component after bandpass filter of 1 –3 Hz is applied. Velocity change of subsurface structure was calculated by applying the stretching method (Sens-Schönfelder and Wegler, 2006) to the ACFs for lag times of 1 –5 s and 4 –15 s.

The results using the lag time of 1 –5 s showed velocity increase of 6 % at the N.MSIH station located near the fault just after the Kumamoto earthquakes. This velocity increase remained more than 6 months. The stations of N.OGNH and N.KKCH also showed velocity increase although the velocity increases completely recovered (disappeared) 6 months after the earthquakes. On the other hand, significant velocity decreases from 0.5 % to 6.0 % were obtained at N.ASVH, N.NMNH, and N.TYNH. The decrease recovered partially except for the N.ASVH. The result for the lag time of 4 –15 s showed velocity decreases from 0.5 % to 6 % at N.MSMH, N.TYNH, N.ASVH, N.HKSH, N.NMNH, N.KKEH, and N.SNIH near the after shock area and a induced seismicity area of the 2016 Kumamoto earthquakes.

The N.MSIH station which showed the velocity increase is located where negative volume change was expected by a theoretical fault model of the Kumamoto earthquakes. Actually, a large compressional strain was observed between the KiK-net sensors installed on the surface and at the borehole bottom at N.MSIH (Fukuyama and Suzuki, 2016). We, therefore, suppose that the velocity increase found only near the fault was caused by the static compressional-strain. On the other hand, the velocity decrease found at several stations in wider area would be caused by large dynamic strain-change.

Keywords: The 2016 Kumamoto Earthquakes, Temporal velocity change

# Temporal Variation in Seismic Velocity Accompanied by 2011 Tohoku-Oki Earthquake and the Slow Slip Event, on Seismic Interferometry of Ambient Noise

\*Miyuu Uemura<sup>1</sup>, Yoshihiro Ito<sup>2</sup>, Kazuaki Ohta<sup>2</sup>, Ryota Hino<sup>3</sup>, Masanao Shinohara<sup>4</sup>

1. Kyoto University, 2. Disaster Prevention Research Institute, Kyoto University, 3. Tohoku University, 4. Tokyo University

Seismic interferometry is one of the most effective techniques to detect temporal variations in seismic velocity before or after a large earthquake. Some previous studies have been reported on seismic velocity reductions due to the occurrences of large earthquakes (e.g., Wegler et al., 2009; Yamada et al., 2010) and preceding them (e.g., Lockner et al., 1977; Yoshimitsu et al., 2009). However, only a few studies accompanying slow slip events have been conducted.

Between the end of January and the occurrence of the largest foreshock on March 9 that preceded the 2011 Tohoku-Oki earthquake, slow slip events and low-frequency tremors were detected off Miyagi (Ito et al., 2013, 2015; Katakami et al., 2016). We apply seismic interferometry using ambient noise to data from 17 OBSs that were installed above the focal region before the 2011 Tohoku-Oki earthquake. All OBSs with three components are short-period seismometers with an eigenfrequency of 4.5 Hz that were deployed off Miyagi between November 2010 and April 2011. Before the analysis, we estimated the original deployment orientation with two horizontal components for 13 OBSs, by using particle orbits of some direct P waves from natural earthquakes, to analyze one vertical and two horizontal components. The method is as follows. First, we applied a band-pass filter of 0.25-2.0Hz in the frequency domain, and compared this with a one-bit technique in the time domain to the ambient noise signal. Second, we calculated Auto-Correlation Coefficients using a 5-s time window with lag time from -30 s to 30 s at intervals of 0.1 s, using seven continuous days of waveforms to make a daily ACF. Third, we stacked up all daily ACFs for the entire time period, to make a reference ACF. Finally, we calculated the Correlation Coefficients between the one-day ACF or the 16-day ACF and the reference ACF.

The results are follows. At all OBSs, the 16 days' CC declined after the SSE initiated and then it recovered in the latter half of the SSE duration. In the region of SSE occurrence, the difference between the absolute and incremental reduction in the 16 days' CC is small. However, in the area of the largest foreshock, the difference is significant. The former 16 days' CC values are suddenly decreasing before the SSE, and the latter 16 days' CC values are gradually decreasing starting around November, or around four months before the largest foreshock. The small difference could be related to the occurrence of SSE, while the large difference could be related to critical conditions preceding the largest foreshock.

Keywords: seismic interferometry, ambient noise



# Estimation of seismic velocity changes in response to the earth tide: Noise correlation analysis at 13 active volcanoes in Japan

\*Tomoya Takano<sup>1</sup>, Takeshi Nishimura<sup>1</sup>, Hisashi Nakahara<sup>1</sup>

1. Graduate School of Science, Tohoku University

Seismic velocity changes due to a large earthquake have received much attention in recent years to understand the mechanical properties of the shallow structure. Strong motion and stress changes due to crustal deformation are considered as mechanisms of seismic velocity changes, however it is necessary to estimate each contribution to understand the mechanism of velocity change quantitatively. Recently, Takano et al. [2014] and Hillers et al. [2015] estimated velocity changes due to the Earth tide by applying seismic interferometry method to ambient noises to investigate the seismic velocity changes only due to stress. However, there are only two studies, hence we estimate seismic velocity changes in response to the Earth tide using ambient noises recorded at 13 active volcanoes in Japan.

Vertical component of ambient noises recorded by Japan Meteorological Agency at 13 active volcanoes in Japan are analyzed: Tokachidake, Meakandake, Mt. Tarumae, Mt. Usu, Hokkaido-komagatake, Mt. Azuma, Mt. Bandai, Nasudake, Mt. Kusatsushirane, Mt. Ontake, Izuoshima, Miyakejima, Unzenfugendake. We analyzed continuous data for 2 years (2013-2014). For every possible pair combination of stations whose distances are within about 5km, we computed cross correlation functions (CCFs) at dilatational and contractional episodes, respectively. Each episode is defined by dividing observation period according to tidal strain amplitudes computed by GOTIC2 [Matsumoto et al., 2001]. CCFs are then stacked for the dilatational episode and the contractional one. By measuring the phase difference between dilatational CCFs and contractional CCFs, seismic velocity changes due to the Earth tide are estimated. Record sections of CCFs indicate that surface wave might be dominant in ambient noise.

Seismic velocity changes due to vertical component of the Earth tide averaged for all station pairs are estimated to be  $-0.02 \pm 0.02\%$  at 0.5-1Hz,  $-0.01 \pm 0.01\%$  at 1-2Hz, and  $-0.06 \pm 0.01\%$  at 2-4Hz, respectively, while seismic velocity changes due to areal component are estimated to be  $0.03 \pm 0.02\%$  at 0.5-1Hz,  $0.02 \pm 0.01\%$  at 1-2Hz, and  $0.06 \pm 0.01\%$  at 2-4Hz, respectively. Negative values of velocity changes indicate seismic velocity is reduced during the dilatational episode in contrast to the contractional episode. Therefore, it appears that seismic velocity is reduced due to vertical dilatation. It is consistent with the result of Hillers *et al.* [2015]. However, Yamamura et al. [2003] and Takano et al. [2014] detected velocity reduction due to areal dilatation. The two studies analyzed P-wave, while this study and Hillers et al. [2015] analyzed Rayleigh waves. This suggests that the observed velocity changes may differ for the orientation of strain and type of seismic waves analyzed.

Keywords: seismic velocity change, seismic interferometry, earth tide

## Globally optimized finite difference method to minimize the angle dependent numerical dispersion.

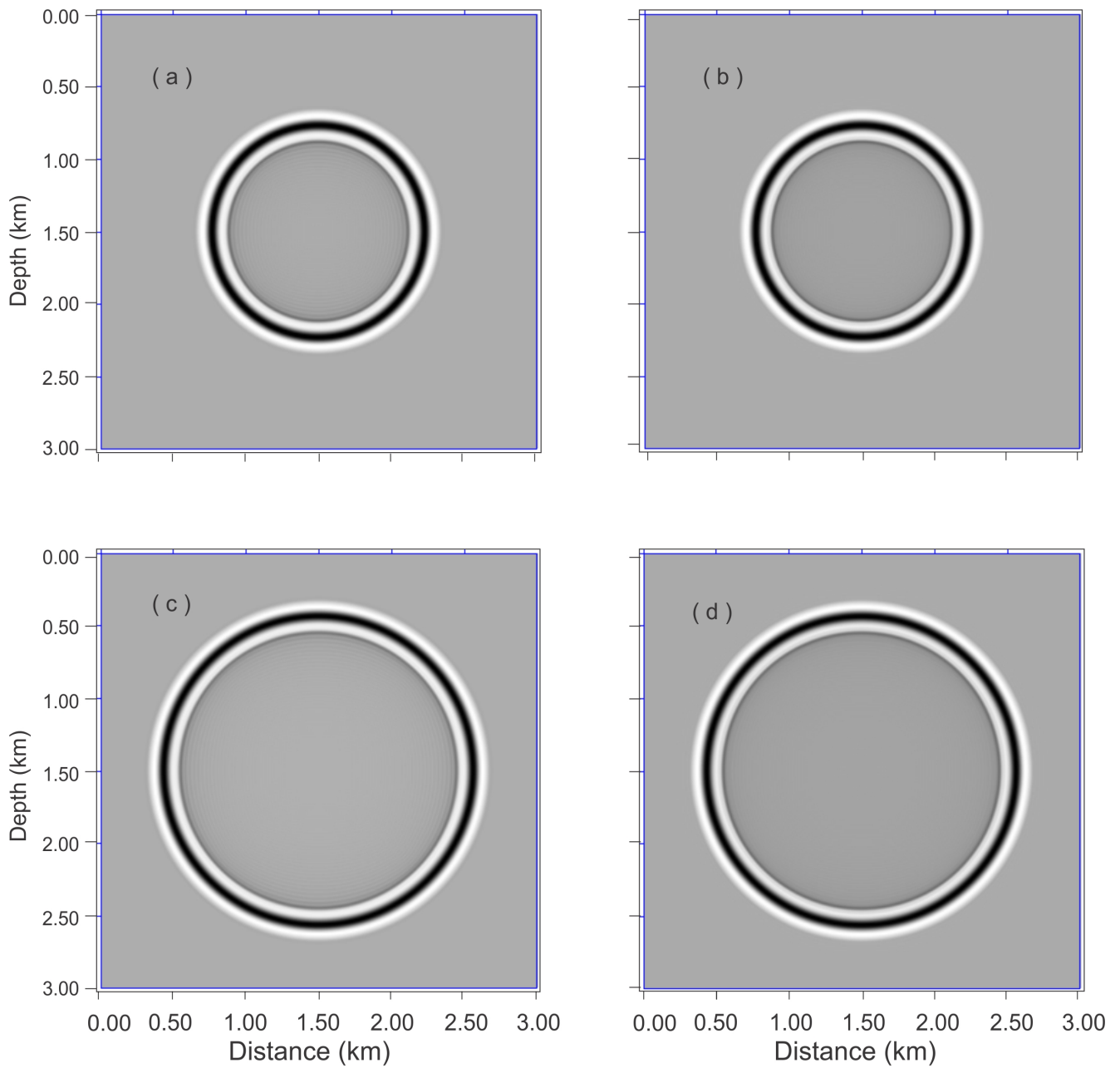
\*DEBAJEET BARMAN<sup>1</sup>, Dr. MAHESWAR OJHA<sup>1</sup>

1. CSIR National Geophysical Research Institute Hyderabad, India

Finite difference modeling is a basic and important tool to solve a differential equation like acoustic wave equation. This method is also used in high resolution seismic imaging. But it faces some challenges for two dimensional wave propagation due to propagation angle dependent numerical dispersion in square grid system. In a conventional Finite Difference Method (FDM), the coefficients are fixed for 1D and 2D propagation. So, with increase of order of approximation the dispersion may be reduced but the non uniformity of dispersion with varying propagation angle retains itself. For existing Pseudo Spectral Method (PSM) using specific window parameter the FD coefficients are constant and is not properly optimized for every angle of propagations.

Here, we propose a method to automatically optimize FD coefficients for every propagation angle. To make the method robust, at first FD coefficients for every propagation angle is optimized by minimizing phase velocity ratio error with reference to the analytic solution using genetic algorithm of certain initial population. Here, the fitness function is generated by the weighted average error in phase velocity ratio for each wave number. As we know that the error in lower wave number should be in higher priority, so we use decay type functions like linear, exponential to calculate the weighted average error by multiplying the function weight with the error at specific wave number. The stability criteria is considered for choosing best of optimized FD coefficients i.e. the FD coefficients whose stability ratio is higher than conventional is considered for the next step for the algorithm. Then final FD coefficients are generated by optimizing from those highly optimized FD coefficients for each propagation angle by genetic algorithm. In the second step, the same stability criteria technique is used for optimization. In second step the FD coefficients are optimized by using fitness function where error is average for every propagation angle. The new method is automated and it does not depend on specific window property like Pseudo Spectral Method (PSM). For some acoustic model PSM technique does not better result for lower order approximation and use of higher order approximation increase the complexity of the method. But in new method there is no such limitation.

Keywords: Genetic algorithm, Phase velocity ratio, Decay function



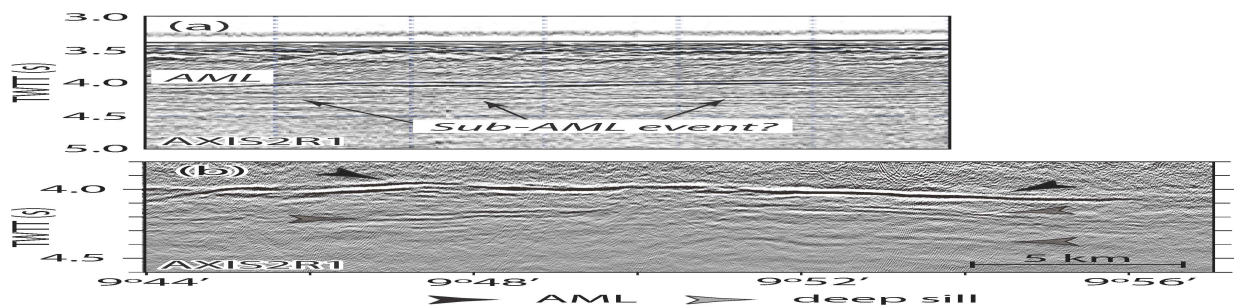
# Waveform modeling of the seismic response of a mid-ocean ridge axial melt sill

\*Min Xu<sup>1</sup>, Wen Yan<sup>1</sup>

1. SCSIO, CAS

Seismic reflections from axial magma lens (AML) are commonly observed along many mid-ocean ridges, and are thought to arise from the negative impedance contrast between a solid, high-speed lid and the underlying low-speed, molten or partially molten (mush) sill. The polarity of the AML reflection ( $P_{AML}P$ ) at vertical incidence and the amplitude versus offset (AVO) behavior of the AML reflections (e.g.,  $P_{AML}P$  and  $S$ -converted  $P_{AML}S$  waves) are often used as a diagnostic tool for the nature of the low-speed sill. Time-domain finite difference calculations for two-dimensional laterally homogeneous models show some scenarios make the interpretation of melt content from partial-offset stacks of  $P$ - and  $S$ -waves difficult. Laterally heterogeneous model calculations indicate diffractions from the edges of the finite-width AML reducing the amplitude of the AML reflections. Rough seafloor and/or a rough AML surface can also greatly reduce the amplitude of peg-leg multiples because of scattering and destructive interference. Mid-crustal seismic reflection events are observed in the three-dimensional multi-channel seismic dataset acquired over the RIDGE-2000 Integrated Study Site at East Pacific Rise (EPR, cruise MGL0812). Modeling indicates that the mid-crustal seismic reflection reflections are unlikely to arise from peg-leg multiples of the AML reflections,  $P$ -to- $S$  converted phases, or scattering due to rough topography, but could probably arise from deeper multiple magma sills. Our results support the identification of Marjanovic et al. (2014) that a multi-level complex of melt lenses is present beneath the axis of the EPR.

Keywords: East Pacific Rise, Axial melt lens, Waveform modeling, Mid-crustal seismic reflection event, Multiple-sill model



# Adjoint tomography beneath the Kanto region using broadband seismograms

\*Takayuki Miyoshi<sup>1</sup>

1. Earthquake Research Institute, University of Tokyo

The three-dimensional seismic structure in the Kanto region of Japan has been revealed in many past studies, whereas no model with the ability to reproduce observed waveforms is available to aid in the tectonic interpretation of the heterogeneity of the region. We have inferred the three-dimensional seismic wave-speed structure using adjoint tomography (e.g. Miyoshi et al. 2015 SSJ; Miyoshi 2016 JpGU). I report here revised results using the modified procedure from the manner of Miyoshi (2016).

The revisions were following three. (1) I re-determined centroid time. I basically used the parameters of MT solutions provided by the NIED F-net as initial source parameters. Although the synthetics are similar with the observation, the synthetic was faster than the observation on almost seismograms due to significant rupture duration. I estimated the centroid time using the differential time between observation and synthetic estimated by phase correlation for a packet of P-waves. (2) I considered attenuation effect in the forward modeling. I assumed attenuation structure depending on S-wave structure (Olsen et al. 2003). (3) I broaden the period band toward shorter periods. I used four period bands between 5 and 30 sec in the iteration. I started the inversion from the waveforms in the period band of 20 - 30 sec, and finally 5 - 30 sec in order to avoid cycle skipping.

One iteration involved forward modeling, estimation of misfit, calculation of misfit kernel using adjoint method, and model update using Hessian kernels. I obtained the preferred model after 16 iteration. Initial model was the tomographic model based on ray theory (Matsubara and Obara 2011). The main results are as follows: (i) the synthetic waveforms improved 20 % based on the amplitude misfit between observation and synthetics in the period of 5 - 30 sec. The new model reproduced the waveforms of both inversion data and extra data well. (ii) As for average wave-speeds in each depth, the average S-wave speed is not changed basically, while the P-wave speed model was slightly slower than that of the initial model. (iii) I detected the extreme low wave-speed areas at a depth of 5 km and 40 km. These low wave-speed areas are consistent with geological and tectonic features pointed out by the previous researches (e.g. Suzuki 1996; Kamiya and Kobayashi 2000).

Acknowledgements: We thank to the NIED F-net for providing seismological data, and the Computational Infrastructure for Geodynamics (CIG) for providing SPEC-FEM3D\_Cartesian code. This work was supported by JSPS KAKENHI (Grant Number 16K21699) and MEXT KAKENHI (Grant number 15H05832).

Keywords: Seismic wave-speed model, Adjoint tomography, Broadband seismogram

# Global features of slabs inferred from regional low- and high-frequency body waves of deep earthquakes

\*Yuki Ohata<sup>1</sup>, Keiko Kuge<sup>1</sup>

1. Department of Geophysics, Graduate School of Science, Kyoto University

We show that high-frequency P and S phases from deep earthquakes arrive at fore-arc stations after low-frequency phases, with increasing delay with thermal parameters in subduction zones. The observation in Tonga may be associated with the metastable olivine wedge (MOW) as well as in northern Japan.

By analyzing features of P and S waves radiated by deep earthquakes, we can elucidate the nature of slabs where the seismic waves have passed. One of the features is difference in arrival time between low-frequency ( $f < 0.25$  Hz) and high-frequency ( $f > 2$  Hz) signals. This can be observed clearly in the fore-arc side of the volcanic front in northern Japan. Furumura and Kennett (2005) showed that the P and S waves from deep earthquakes beneath the Sea of Japan have low-frequency onsets with high-frequency long-duration signals, suggesting that they are the result of small-scale quasi-laminar heterogeneity within the subducting Pacific slab. The late arrivals of high-frequency P and S signals can be enhanced for earthquakes deeper than 400 km due to the low-velocity MOW in the slab (Furumura et al., 2016).

In this study, we examined seismograms worldwide for the features suggested by Furumura's studies. We collected waveform data of P and S waves from IRIS and F-net broadband seismometers in fore-arc sides of subduction zones where deep earthquakes occur. We measured separation time between low- and high-frequency arrivals. By comparing it with several physical parameters of subduction zones, we found that the separation time could increase with the thermal parameter. The result is consistent with Kennett et al. (2014) who suggested that the quasi-laminar heterogeneity within the oceanic lithosphere can guide high-frequency  $P_o$  and  $S_o$  waves more efficiently in the older, cold areas of the Pacific. Therefore, the observed correlation between the separation time and thermal parameter may arise from the dependence of the quasi-laminar heterogeneity on temperature. In the areas except for Tonga and northern Japan, we did not find observations that are likely to be evidence for MOW. Large separation time was observed in Tonga, and it tends to be increased for earthquakes deeper than 500 km.

# The cause of $M_j$ overestimates ( $M_j > M_w$ ) for the shallow earthquakes in western Japan

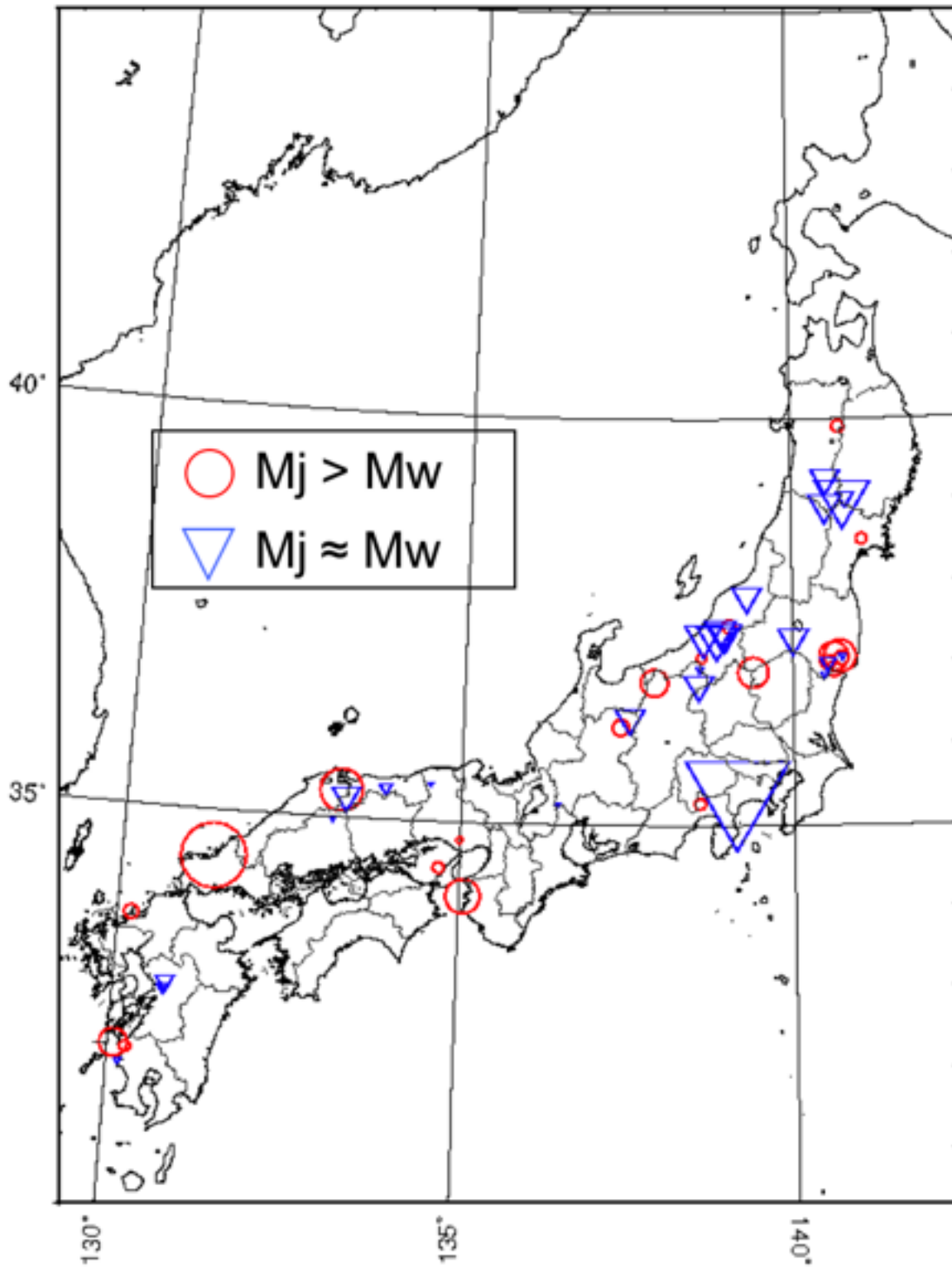
\*Hiroki Kawamoto<sup>1</sup>, Takashi Furumura<sup>1</sup>

1. Earthquake Research Institute The University of Tokyo

In Japan, the Japan Meteorological Agency (JMA) magnitude ( $M_j$ ) is officially used for the magnitude estimates of the earthquakes occurring in the area around Japan. However, it is well recognized that the estimated  $M_j$  sometimes shows large discrepancies between the moment magnitude ( $M_w$ ) and momentum magnitude ( $M_w$ ). Typical examples are the Western Tottori earthquake in 2000 ( $M_j=7.3$ ;  $M_w=6.8$ ) and Northern Yamaguchi earthquake in 1997 ( $M_j=6.6$ ;  $M_w=5.9$ ), all are strike-slip fault events occurred in the inland of western Japan. Since the  $M_j$  of shallow ( $h < 60$  km) earthquakes are estimated by using the maximum amplitude of horizontal displacement motions recorded by long-period seismometers with a natural period of  $T=5$  s, it is expecting that the propagation and attenuation properties of the long-period ground motions in this period range might be different in western Japan. In this study we examined the cause of such discrepancy between  $M_j$  and  $M_w$  occurring in western Japan based on the analysis of the K-NET and KiK-net strong ground motion data for recent shallow earthquakes.

We analyzed 47 inland earthquakes of shallow ( $h < 40$  km) and large ( $M_j > 5.5$ ) event occurred during between Sep. 1994 to Nov. 2016 in which the K-NET and KiK-net data is available. We made a regression analysis of relation between  $M_j$  and  $M_w$ , which are obtained from the JMA and the GCMT catalog, respectively. The result shows that the  $M_j$  is proportional to the  $M_w$  with a bias of 0.16 ( $M_j=M_w+0.16$ ). After substituting this bias (0.16) from the  $M_j$  we selected the events having large discrepancy between  $M_j$  and  $M_w$ . We confirmed such peculiar events are mostly located in some area such as in Chugoku-Kinki and from South-Fukushima to South-Niigata (Fig).

To study the cause of larger  $M_j$  than  $M_w$  in western Japan we examined the strong motion record of the K-NET and KiK-net for the 2000 Western Tottori ( $M_j=7.3$ ;  $M_w=6.8$ ) and the 2004 Mid Niigata ( $M_j=6.8$ ;  $M_w=6.8$ ) earthquakes. The accelerograms of the K-NET and KiK-net are integral twice to obtain the ground displacement after applying a band pass filter ( $f=0.20$  to 40 Hz) to match to the response of the JMA seismograph. Obtained waveform shows that the attenuation of the long-period ground displacement motion from the Mid Niigata earthquake is very strong with propagation in northern Japan, but it is rather weak for the Western Tottori earthquake in western Japan. It is also confirmed that the large ground displacement of the Western Tottori earthquake has strong directional dependency with larger tangential motion in the direction of fault strike and its perpendicular directions where the radiation of the SH wave from the strike-slip fault source develops large Love waves. The seismogram demonstrated that the Love wave traveling longer distances in western Japan without showing strong dispersion properties, while the development of the surface wave from the Mid Niigata earthquake is very weak in all directions. The results of this study demonstrated that the earthquakes of larger  $M_j$ , which occurred in western Japan, might be due to larger radiation of the Love wave from the source as well as efficient propagation of the short-period ( $T=5$  s) Love wave in regional distances without causing significant dispersion. Such efficient Love wave propagation in western Japan might indicate the peculiarity of the crustal structure beneath western Japan compared with that of northern Japan. Such propagation and dispersion properties of the fundamental-mode, short-period ( $T=5$  s) Love wave might occur due to the difference in the shallow structure such as sedimentary layers between western and northern Japan.





# Numerical simulation of long-period ground motion generated from intraplate earthquakes around Ibaraki and Fukushima prefectures ~ Part III

\*Fujihara Satoru<sup>1</sup>, Fumio Kirita<sup>2</sup>, Kaoru Kawaji<sup>1</sup>, Toshihiko Yamazaki<sup>2</sup>, Mitsuru Uryu<sup>2</sup>, Daisuke Takekawa<sup>2</sup>

1. CTC ITOCHU Techno-Solutions, Nuclear & Engineering Department, 2. Japan Atomic Energy Agency, Construction Department

[Introduction] After the occurrence of 2011 Tohoku-Oki earthquake, phenomena of long period ground motion have been observed at seismic observation stations around the coastal region of Ibaraki prefecture for the occurrence of shallow depth intra-plate earthquakes (including 2011 Fukushima-ken Hamadori Earthquake) around Ibaraki and Fukushima prefectures. Before the occurrence of Tohoku earthquake, there was little noticeable intraplate large earthquake, and physical characteristics of generation of long-period ground motion mostly remained unclear. Therefore, better understanding nature of generation of long-period ground motion and improving seismic wave propagation around this region are very important for evaluating ground motion around the coastal region of Ibaraki prefecture. They will also lead to more reasonable evaluation of earthquake-proof safety of important infrastructures and subsurface structure around this region.

[Previous studies] In our previous studies, for achieving more accurate evaluation of seismic wave ground motion of intra-earthquakes around the coastal region of Ibaraki prefecture (strong motion, long-period ground motion, and etc), the 3-D underground structure model, which fairly explains phenomena of long-period ground motion, has been reconstructed by using postseismic events of 2011 Hamadori Earthquake. For optimizing the 3D underground structure model, we used seismic observation stations of KIK-net and Japan Atomic Energy Agency around this region. The result showed that optimized 3D structure model could better explain the generation of long-period ground motion around this region, and suggested that they are generally originated from the regional-scale characteristics of basement structure beneath intra region. Furthermore, based the finite element method using on the structure model, we performed seismic wave propagation simulation of intraplate earthquakes (moderate scale of point source,  $M < 6.0$ ), and try to forward-model the long-period ground motion being generated during propagation thorough the inhomogeneous underground structure. Preliminary results were presented in the 2015 JPGU and 2016 JPGU.

[What we will show in this presentation] This presentation introduces the updated results our research as follows; (1) Validation tests of the 3-D underground structure model for large-scale earthquakes with finite fault model setting. We analyze several models of 2011 Hamadori Earthquake. (2) We also analyze several specific propagation properties. These include amplitude fluctuations possibly affected by source-station azimuth, source depth, specific frequency band, and so on.

Keywords: 3D structure, Seismic wave propagation, Hamadori Earthquake